Mechanism of Adsorption of Cadmium and Lead Ions by Iron-activated Biochar

Liqiang Cui,[a] Tianming Chen,[a] Chuntao Yin,[a] Jinlong Yan,[a,*] James A. Ippolito,[b] and Qaiser Hussain [c]

Heavy metal removal from aqueous matrices may help reduce disease and cancer incidences. In this study, reed biochar (RBC) and RBC modified by ferrous ammonium sulfate addition (1 mol Fe L^{-1}) were compared for potential Cd and Pb removal from varying pH aqueous solutions. Surface functional groups were identified using Fourier transform infrared (FTIR) analysis, and their surface physicochemical structure was observed using scanning electron microscopy-energy dispersive spectrometry (SEM-EDS). Batch experiments showed that the modified-reed biochar (MRBC) had greater Cd and Pb removal capacities over a wide pH range (1 to 8), as well as greater metal sorption capacities compared to RBC. Metal reaction kinetics occurred relatively quickly (*i.e.*, within 60 min), and Langmuir modeling suggested that Cd and Pb removal by MRBC was maximized at 2.97 mg g^{-1} and 17.5 mg g^{-1} at 45 °C, respectively. The MRBC effectively sorbed Cd and Pb likely due to associations with functional groups modified by the Fe addition. In the future, MRBC may be used as an efficient and eco-friendly adsorbent for Cd and Pb removal from aqueous solutions and may help reduce water-borne issues associated with metal contamination.

Keywords: Biochar; Reed biochar; Heavy metals; Amendment; Contaminated water

Contact information: a: School of Environmental Science and Engineering, Yancheng Institute of Technology, No. 211 Jianjun East Road, Yancheng 224051, China; b: Department of Soil and Crop Sciences, Colorado State University, Fort Collins, Colorado 80523, USA; c: Department of Soil Science and Soil Water Conservation, PirMehr Ali Shah Arid Agriculture University, Rawalpindi, Pakistan;
 * Corresponding author: yjlyt4788@126.com

INTRODUCTION

Industrial effluents from smelting facilities, dye factories, and paper mills contain various heavy metals that can be responsible for surface water, groundwater, and soil contamination. Once in water or soil, heavy metals can be transferred and accumulated into edible plant parts, becoming part of the food chain, and thus pose a threat to public health (Khan *et al.* 2008). Specifically, heavy metals such as cadmium (Cd) and lead (Pb), are well known pollutants that cause diseases such as itai-itai, Minamata disease, and various cancers (Harada 1995; Bolognesi *et al.* 1999; Inaba *et al.* 2005; Khan *et al.* 2014). Because of the negative connotation between heavy metals, health risk, and the environment, several amendment methods and technologies have been used for the removal/stabilization of heavy metals from wastewaters and soil (Bogusz *et al.* 2015). Traditional metal removal methods include chemical precipitation, ion exchange, and membrane separation processes (Chen *et al.* 2015). Unfortunately, some of these methods and technologies require special facilities to remove such metals as well as expensive chemicals to remove these metals or follow more complex processes, making traditional

metal removal methods less attractive for environmental cleanup. Simpler heavy metal sorbents are needed that ideally come from local sources near local heavy metal problem areas.

Biochar, a carbon-rich byproduct derived from biomass pyrolysis under oxygen-limited conditions (Wang *et al.* 2016), shows significant promise as a heavy metal sorbent (Mohan *et al.* 2014; Kim *et al.* 2015; Ippolito *et al.* 2017). Ippolito *et al.* (2017) found that pine biochar can reduce bioavailable soil metals (Cd, Cu, Pb, and Zn), which were extracted with 0.01 M $CaCl_2$. Uchimiya *et al.* (2010) used biochar to immobilize several metals (Cu, Cd, Ni, and Pb) from an aqueous solution. Pig and cow manure biochars have been demonstrated to be efficient sorbents for removing Cu(II), Zn(II), Cd(II), and Pb(II) ions from an aqueous solution (Kołodyńska *et al.* 2012). Bamboo biochar has been shown to be an efficient sorbent for Pb and Cd removal from aqueous solutions. Also, the quantity of Pb sorbed is reduced when both metals are present together in solution (Han *et al.* 2017), suggesting that competitive metal sorption likely occurs on biochars. These studies utilized biochars in a non-activated (*i.e.,* as-is) state, yet studies have shown that activating biochar may increase heavy metal sorption over non-activated biochars.

Karunanayake *et al.* (2018) found that Fe_3O_4-magnetized Douglas fir biochar is effective sorbed Cd and Pb and easy separated from aqueous solution. Steam-activated (800 °C for 3 h) and KOH-treated (1.3 M) biochars have been shown to successfully remove Cu from solutions (Ippolito *et al.* 2012). Similarly, modified biochars (nanoscale zerovalent, NaOH, and Zn ion-modified biochars) produced from various metal ion-treated biomass materials are used as adsorbents for heavy metal (Cd, Pb, As, *etc.*) removal from water (Wang *et al.* 2017). Biochar modification *via* activation can increase surface area, ligand functional group presence, or the amount of C = C π electrons available (Uchimiya *et al.* 2010; Ippolito *et al.* 2012; Qiao *et al.* 2015), all of which play a role in improving heavy metal sorption.

Reed (*Phragmites australis*), a halophyte in coastal areas, is widespread in many saline-alkali lands and aquatic ecosystems in China (Zheng *et al.* 2013). Reed has tolerance to salts and floods, is used to improve soil conditions, and grows relatively quickly, making it a suitable raw material for biochar production (Roberts *et al.* 2010). In this study, a modified reed biochar was synthesized *via* pretreatment with ferrous ammonium sulfate [$(NH_4)_2Fe(SO_4)_2$] for the eventual removal of solution-borne Cd and Pb.

It was hypothesized that biochar pretreatment with a strong reducing agent, $(NH_4)_2Fe(SO_4)_2$, could be a precursor for amorphous iron oxide (FeOx) formation, which following pyrolysis could enhance biochar reactive surfaces and improve biochar's ability to remove Cd and Pb from a solution. Thus, the objective of this study is to investigate the efficacy of reed-derived biochar (RBC) compared to modified reed-derived biochar (MRBC) for removing and retaining Cd and Pb from an aqueous solution. Finally, biochar Cd and Pb sorption mechanisms are elucidated by examining functional group presence using Fourier transform infrared (FTIR) and microscopic physico-chemical structure using scanning electron microscopy-energy dispersive X-ray spectroscopy (SEM-EDS).

EXPERIMENTAL

Materials

Reed (*Phragmites australis*) was collected from a beach at Yancheng in Jiangsu, China. The collected reed samples were washed with tap water, triple rinsed with distilled water, dried at 60 °C, and then powder ground. Biochar was made from reed powder pyrolyzed at 450 °C for 4 h with a linear rise of 10 °C min^{-1} in a vacuum tube furnace (NBD-O1200; Nobody Material Science and Technology Co., Ltd., Henan, China) and in a nitrogen gas environment (500 mL min^{-1}). After pyrolysis and cooling, biochar was ground passing through 0.15 mm, 0.18 mm, 0.25 mm, 0.42 mm, 0.85 mm, and 2 mm sieves.

The modified reed biochar (MRBC) was made by soaking 250 g of powder reed biomass in 1 L of 1 M $(NH_4)_2Fe(SO_4)_2$ in a 1.5-L plastic bottle with a neutral pH. This solid to liquid ratio filled the plastic bottle with no head space for air. Next, the mixture was shaken at 180 rpm for 24 h at 25 °C, and then the reed biomass was separated *via* filtration. Afterwards, the material was washed with deionized water until the filtrate was free of Fe with loretin testing (Johansson *et al.* 2016). The treated, rinsed reed biomass was oven-dried to a constant weight (24 h, 60 °C), converted to MRBC by slow pyrolysis as the RBC methods, and sieved into the various size fractions described above.

Methods

Basic biochar properties of the 0.15-mm size fraction are presented in Table 1, and were analyzed according to procedures described by Lu (2000), including pH (glass electrode method), carbon (potassium dichromate titrimetric method), total N (Kjeldahl method), total P ($H_2SO_4/HClO_4$ digestion followed by the molybdenum blue method), total K (flame atomic absorption method), and total Cd and Pb (flame atomic absorption spectrometry, FAAS. The specific surface area (SSA) was determined by the Brunauer–Emmett–Teller (BET) method with a surface area and porosity analyzer (ASAP 2460; Micromeritics, Norcross, GA, USA). Biochar cation exchange capacity (CEC) was measured *via* the sodium acetate exchange method. Briefly, the biochar was mixed with an excess of sodium acetate solution, resulting in an exchange of the added sodium cations for the matrix cations. Next, the biochar was washed with 95% alcohol. An ammonium acetate solution was then added, which replaced the adsorbed sodium with ammonium. Finally, the displaced Na was determined through atomic sorption spectroscopy (AAS; TAS-986; Beijing Persee General Instrument Co., Ltd., Beijing, China). Biochar functional groups, such as –OH and C=O, were identified using a FTIR spectrometer (Nexus-670; Thermo Fisher Scientific, Waltham, MA, USA) *via* the KBr (KBr:biochar, 100:1) tablet method.

Table 1. Basic Properties of the 0.15-mm Size Fraction of RBC and MRBC.

	pH	SSA[†]	Carbon	N	P	K	CEC	Cd	Pb
	(H$_2$O)	(m^2 g^{-1})	(g kg^{-1})				(cmol$^+$ kg^{-1})	(mg kg^{-1})	
Reed	/	/	402.5	4.13	2.08	3.92	/	ND	ND
RBC	8.50	5.6	879.1	10.48	26.32	20.35	4.32	0.01	2.17
MRBC	10.53	10.5	812.5	55.65	34.01	19.56	9.34	0.02	3.96

[†] SSA: specific surface area; CEC: cation exchange capacity; the N, P, K, Cd, and Pb concentrations are expressed as total concentrations; ND: not detected.

bioresources.com

Cadmium (as $CdCl_2$) and Pb (as [$Pb(NO_3)_2$]) (chemicals purchased from Sinopharm Chemical Reagent Co., Ltd., Shanghai, China) sorption onto the biochars was determined as a function of solution pH. The 0.15-mm RBC or MRBC size fraction was used (as this fraction sorbed the greatest metal concentrations as per the above experiment) with 0.10 g biochar mixed with 50 mL of 0.01 M $NaNO_3$ solution containing either 5 mg Cd L^{-1} or 50 mg Pb L^{-1}. The solution pH was either 1, 2, 3, 4, 5, 6, 7, or 8, which was adjusted using either 0.1 mol L^{-1} HCl or NaOH before shaking. All treatments were replicated three times. The solutions were then shaken for 2 h at 180 rpm, filtered, and the filtrate Cd and Pb concentrations were determined by AAS.

Next, Cd and Pb sorption experiments were conducted using both RBC and MRBC in batch equilibrium experiments at 25 °C. First, Cd and Pb sorption onto the various biochar size fractions (*e.g.*, 0.15, 0.18, 0.25, 0.42, 0.85, and 2 mm) was determined to identify the ideal size fraction for the greatest metal sorption capability. Three 0.10 g RBC or MRBC samples were mixed with 50 mL of 0.01 M $NaNO_3$ solution containing either 5 mg Cd L^{-1} or 50 mg Pb L^{-1} with a natural pH (approximately 7). The mixtures were shaken for 2 h at 180 rpm, filtered, and the filtrate Cd and Pb concentrations were determined by AAS.

Next, the biochar dose necessary to maximize Cd or Pb sorption was determined. The 0.15-mm RBC or MRBC size fraction was again used, with either 0.08, 0.10, 0.20, 0.40, or 0.80 g biochar mixed with 50 mL of 0.01 M $NaNO_3$ solution containing either 5 mg Cd L^{-1} or 50 mg Pb L^{-1} with a natural pH (approximately 7). All treatments were replicated three times. The mixtures were shaken for 2 h at 180 rpm, filtered, and the filtrate Cd and Pb concentrations were determined by AAS.

Sorption kinetics were then determined only for the MRBC. Three, 0.10 g biochar samples from the 0.15-mm size fraction were mixed with 50 mL of 0.01 M $NaNO_3$ solution containing either 5 mg Cd L^{-1} or 50 mg Pb L^{-1}; the solution pH was not controlled. These experiments were performed at 25 °C, 35 °C, and 45 °C in a water bath with varying shaking times (0, 10, 30, 60, 120, 240, and 480 min). All of the solutions were then filtered and analyzed for their Cd and Pb concentrations using AAS.

Biochar equilibrium isotherms were also only determined for the 0.15-mm MRBC size fraction. Three, 0.10 g biochar samples were mixed with 50 mL of 0.01 M $NaNO_3$ solution containing increasing Cd (0, 1, 2, 8, 10, 20, and 40 mg Cd L^{-1}) or Pb (0, 20, 40, 80, and 160 mg Pb L^{-1}) concentrations. The mixtures were shaken for 2 h at 180 rpm and at 25 °C, 35 °C, and 45 °C in a water bath; the solution pH was not controlled. These metal concentrations bracketed Cd and Pb concentrations that are found in industrial wastewaters (*e.g.*, Singh *et al.* 2016). All of the solutions were then filtered and the filtrate Cd and Pb concentrations were determined by AAS.

Heavy metal RBC and MRBC sorption rate behaviors were evaluated using the pseudo-first-order (1) and pseudo-second-order (2) model equations as follows,

$$ln(Q_e - Q_t) = lnQ_e - K_1 t \tag{1}$$

$$\frac{t}{Q_t} = \frac{t}{Q_e^2 \times K_2} + \frac{t}{Q_e} \tag{2}$$

where Q_e and Q_t are the amounts of the heavy metal sorption capacity per unit weight of biochar (mg g^{-1}) corresponding to the equilibrium and time t (min), K_1 is the pseudo-first-

order constant (h^{-1}), K_2 is the pseudo-second-order constant (g mg^{-1} h^{-1}), and the t is time (min).

The prediction models of Freundlich (3) and Langmuir (4) were also employed,

$$lnQ_e \; = \; lnK_F \; + \; \frac{1}{n} \times lnC_e$$

(3)

$$Q_e = \frac{C_e \times K_L \times Q_{max}}{1 + C_e \times K_L}$$

(4)

where C_e is the heavy metal solution concentration (mg L^{-1}) after 2 h, Q_{max} is the maximum adsorption capacity (mg g^{-1}), K_F is the Freundlich parameter related to sorption capacity, K_L is the Langmuir constant (L mg^{-1}) that estimates the binding strength between the surface and the sorbate, and n is an empirical constant.

Finally, the particle composition of RBC and MRBC was determined *via* scanning electron microscopy equipped with energy dispersive X-ray spectroscopy (SEM-EDS; Nova Nano SEM 450; FEI Co., Hillsboro, OR, USA). Biochar SEM-EDS analyses were performed on non-coated particles, directly mounted on an Al SEM-stub using double-sided adhesive copper conducting tape (3M®, Oxford Instruments, Abingdon, UK). The SEM operational conditions used were a 15-kV accelerating voltage at 40 to 90000× magnifications, with back-scattered electrons collected under low vacuum. The EDS elemental spectra were collected from specific locations of interest on both the RBC and MRBC particles.

RESULTS AND DISCUSSION

Characterization of BC

Functional groups present on the RBC and MRBC were compared to that of the powder ground reed feedstock using FTIR (Fig. 1). The reed and modified reed biochar spectra were different when compared to the reed feedstock, with the FTIR spectra reflecting the presence of functional groups due to dehydration, decarbonylation, depolymerisation, and fragmentation during pyrolysis and the activation process (Kan *et al.* 2016). The presence of intermolecular O-H from the dehydration of cellulosic and ligneous components was observed at 3500 to 3200 cm^{-1}. The abundance of C-H (2977 to 2921 cm^{-1}), aliphatic C-O-C (1050 cm^{-1}), and alcohol-OH (1158 cm^{-1}) was attributed to the presence of cellulose.

The increased peak intensities of -OH (3345 to 3426 cm^{-1}) and C-H (3032 to 2858 cm^{-1} and 1452 to 1319 cm^{-1}) and the decreased intensity of aliphatic C-O-C (1050 cm^{-1}) with modified biochar were consistent with dehydration reactions and functional groups changes that occur with temperature changes during the pyrolysis process (Qian *et al.* 2016). Similar to these results, Wang *et al.* (2015) reported that modified-biochar contains more oxygen-containing functional groups and a larger surface area than unmodified biochar. Modified biochar functional groups, such as C-O-C, -OH, C-C, *etc.*, and special microstructures play a vital role in metal sorption by binding or complexing Cd and Pb (Cui *et al.* 2013, 2014; Xu *et al.* 2013).
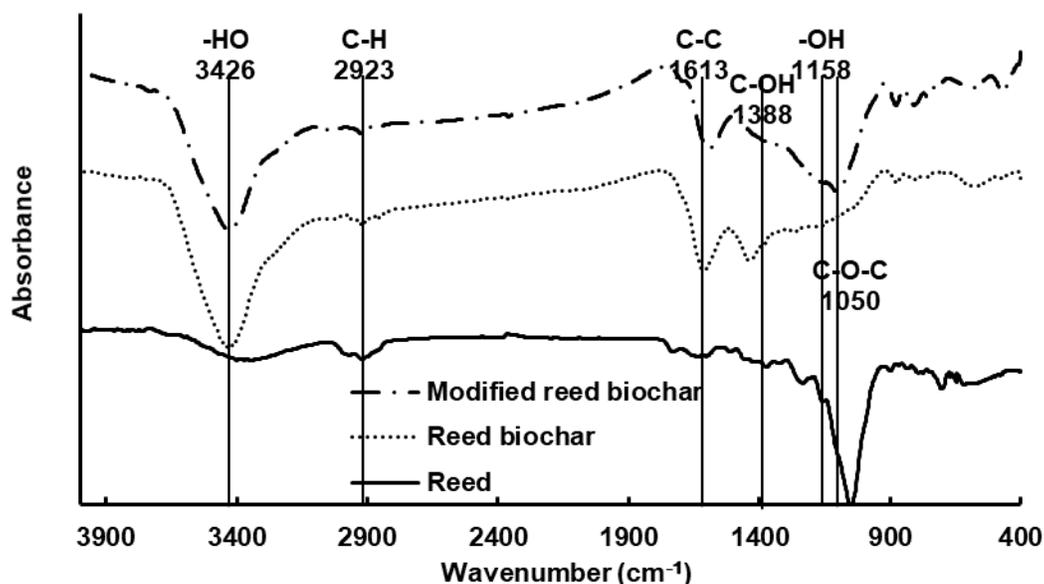
Fig. 1. FTIR spectra of reed, RBC, and MRBC.

Effect of Solution pH

Changing the solution pH remarkably affected the Pb and Cd sorption on both biochars (Figs. 2A and 2B). Over the pH range studied, the Cd and Pb sorption capacities of MRBC increased 7.5% to 41.9% and 6.4% to 59.0% compared to the RBC, with metal removal efficiencies increasing with increasing pH. However, when the pH was greater than 7, the biochar metal removal rates slowed down due to dominating precipitation reactions (Inyang *et al.* 2012; Liang *et al.* 2017). Chen *et al.* (2015) showed that, in the presence of biochar, Cd precipitates as $Cd(OH)_2$ (and Pb likely $Pb(OH)_2$) when the solution pH is greater than 8. Similarly, Ippolito *et al.* (2017) noted that biochar application to acidic mine soils raises the pH, causing Pb to precipitate as hydroxide phases.
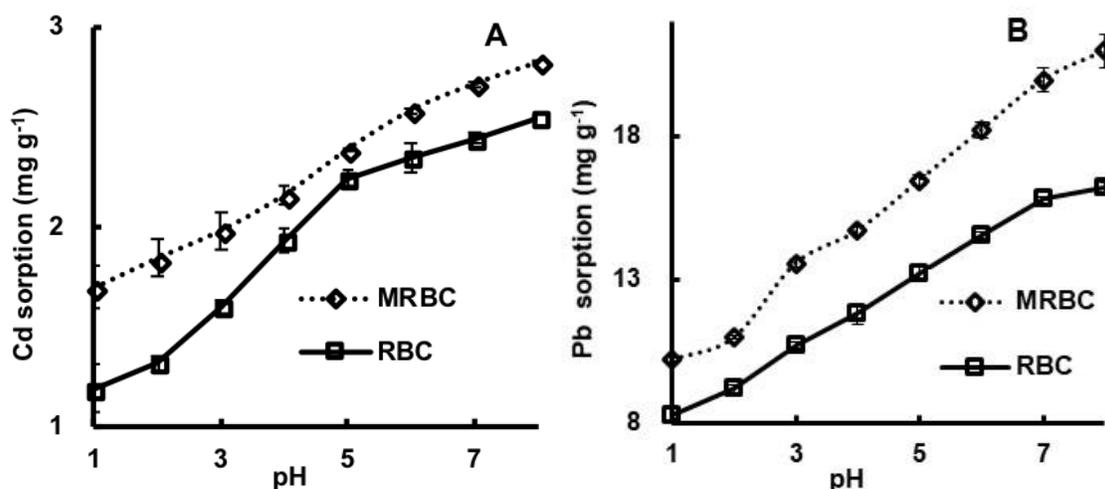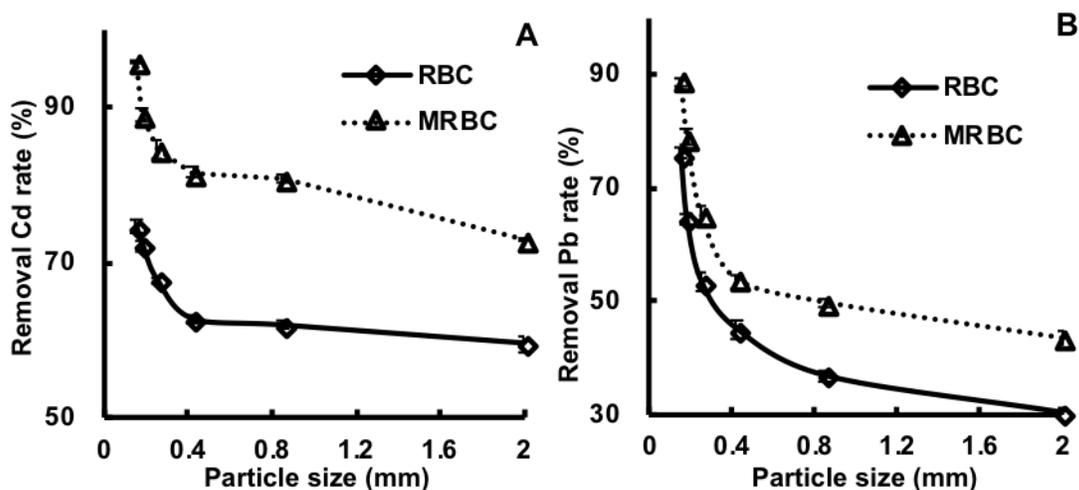

Fig. 2. Effect of 0.10 g from the 0.15 mm size-fraction of MRBC and RCB, mixed with 50 mL of 0.01 M $NaNO_3$ solution containing either 5 mg Cd L^{-1} or 50 mg Pb L^{-1} at initial pH values of 1 to 8, on biochar (A) Cd and (B) Pb adsorption capacities

Others have noted that pH-dependent surface charge plays a vital role in improving biochar metal surface sorption through electrostatic interactions (Cui *et al.* 2014) and metals exchange with cations on biochar, which is commonly considered to reach equilibrium relatively quickly (*e.g.*, Ca^{2+}, Mg^{2+}, and Na^+; Lu *et al.* 2012; Chen *et al.* 2015). In addition to precipitation reactions at elevated pH values, oxygen-containing functional groups (*e.g.*, carboxyl and hydroxyl) on both biochars were likely negatively charged, further enhancing Cd and Pb sorption; Ippolito *et al.* (2017) noted a similar Cd sorption response in the presence of biochar. Thus, Cd and Pb precipitation reactions and electrostatic sorption was enhanced in the MRBC *via* the Fe activation treatment.

## Effect of BC Particle Size and Dosage

Cadmium and Pb solution removal rates increased as the biochar particle size decreased and following biochar activation (Figs. 3A and 3B). Cadmium removal rates ranged from 59.6% to 74.6% (RBC) and 72.9% to 95.9% (MRBC), while Pb removal rates ranged from 30.2% to 76.1% (RBC) and 43.6% to 88.8% (MRBC). The smaller RBC particle size likely contained greater surface area for the metal sorption reactions to occur. Moreover, crushed reed material activated with Fe from $(NH_4)_2Fe(SO_4)_2$ likely enhanced Fe and SO_4^{2-} loading, and in conjunction with small particles and larger surface area, made the MRBC more reactive for Pb and Cd sorption; Han *et al.* (2016) reported a similar observation.

Fig. 3. Effect of 0.10 g of MRBC and RBC mixed with 50 mL of 0.01 M $NaNO_3$ solution containing either 5 mg Cd L^{-1} or 50 mg Pb L^{-1} over biochar particle size (from 0.15 to 2 mm), at a pH of ~7, on (A) Cd and (B) Pb adsorption capacities

Increasing the biochar dose, at a constant initial metal concentration, increased the Pb and Cd sorption onto both the RBC and MRBC (Figs. 4A and 4B). When the biochar dose was increased from 0.08 to 0.8 g 50 mL^{-1}, the Cd removal rate increased from 18.2% to 86.8% (RBC) and 24.2% to 98.3% (MRBC), and the Pb removal rates increased from 23.9% to 83.5% (RBC) and 32.7% to 99.9% (MRBC). Increasing the biochar dosage provided greater quantities of active sites and thus greater heavy metal removal, until the removal efficiency plateaued. Furthermore, the Cd and Pb plateau was greater with MRBC likely due to Fe activation and a subsequent increase in surface area (MRBC > RBC; Table 1). Others have also suggested that biochar activation increases

surface area, leading to greater metal sorption (Lima and Marshall 2005; Azargohar and Dalai 2008; Uchimiya *et al.* 2010).
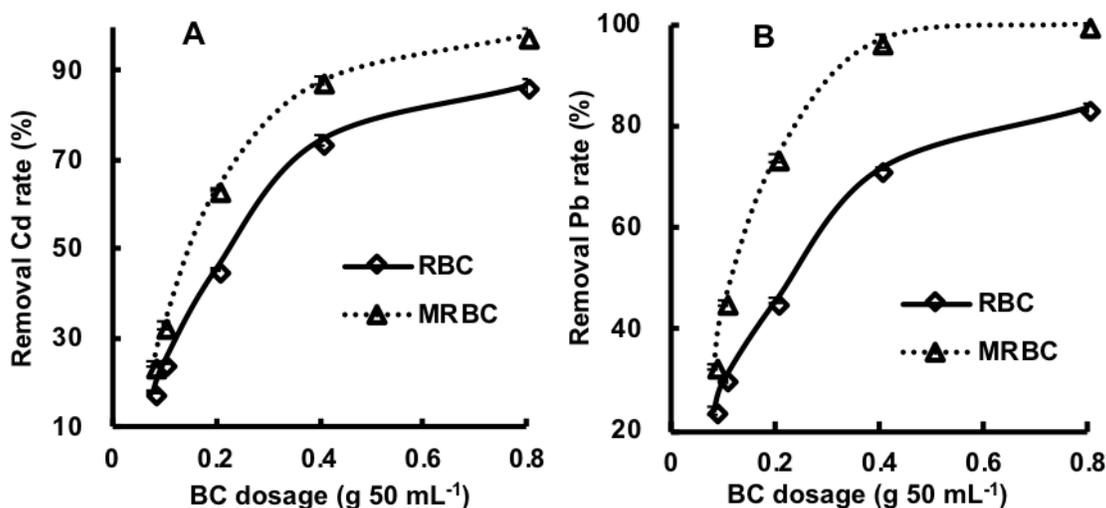
Fig. 4. Effect of MRBC and RBC dose (0.08 to 0.80 g 50 mL^{-1}) from the 0.15 mm size-fraction, mixed with 50 mL of 0.01 M NaNO$_3$ solution (pH approx. 7) containing either 5 mg Cd L^{-1} or 50 mg Pb L^{-1}, on the removal rate of Cd (A) and Pb (B)

MRBC Sorption Kinetics

The MRBC Cd and Pb pseudo-first-order and pseudo-second-order sorption kinetics as related to temperature, and the corresponding degree of fitting values, are shown in Fig. 1S and Table 2, respectively. Across all temperatures, the metal sorption linearly increased for the first approximately 60 min, reaching a plateau after approximately 120 min. Initial, rapid sorption (*i.e.*, first 60 min) may have been attributable to metal-hydroxyl group associations on MRBC outer surfaces. As sorption is slowed (*i.e.*, after 60 min), metal sorption likely shifts from outer to inner MRBC surfaces (Makris *et al.* 2005; Bogusz *et al.* 2015), or due to metal precipitation with Fe-bearing activated phases. This suggests that, over time, Cd and Pb sorption onto MRBC is controlled by a chemisorption process involving precipitation reactions, as observed in other biochar-metals systems (Kołodyńska *et al.* 2012; Bogusz *et al.* 2015). Although not determined in the current study, one cannot rule out: 1) competitive adsorption processes existing between the same and different metals, such as observed for Cd and Pb ions (Han *et al.* 2017) and for Pb, Cd, Zn, Cu, K, and Na (Xu *et al.* 2013); and 2) metal sorption as a second, third, *etc.*, monolayer (Harter and Naidu 2001).

Temperature had an effect on Cd and Pb removal efficiency at the same initial metal ion concentrations (Fig. 1S). The increase in solution temperature, from 25 to 45 °C, led to an increase in MRBC Cd and Pb adsorption capacities. This may indicate that the adsorption process is endothermic (Jung *et al.* 2018). The increase in Cd and Pb removal efficiency with increasing temperature may be due to electrostatic forces between MRBC active sites and metal ions, causing increased sorption from the solution to solid biochar phase (Idrees *et al.* 2018).

Furthermore, greater temperatures also influenced the magnitude of the sorption correlation coefficient (R^2). Cadmium sorption onto MRBC was better fitted to the pseudo-first-order model ($R^2 = 0.993$ to 0.999) than the pseudo-second-order model ($R^2 = 0.966$ to 0.984); the opposite was observed for Pb (pseudo-second-order: $R^2 = 0.976$ to

0.987 as compared to pseudo-first-order: R^2 = 0.936 to 0.958). Pseudo-second-order fitted the data with R^2 values of lower 0.999. Certainly, the higher fitting of kinetic data with the pseudo-first-order model, as temperature was increased, confirmed that Cd and Pb sorption onto biochar were not just a simple particle diffusion as in a first-order reaction (El-Banna *et al.* 2018).

Table 2. Constants and Correlation Coefficients of Pseudo-first-order and Pseudo-second-order Models for Cd and Pb Adsorption by MRBC

Treatments	Temperature	Pseudo-first-order Model		Pseudo-second-order Model	
		K_1	R^2	K_2	R^2
Cd	25 °C	0.037	0.993	0.019	0.966
	35 °C	0.042	0.996	0.022	0.976
	45 °C	0.044	0.999	0.024	0.984
Pb	25 °C	0.113	0.936	0.014	0.976
	35 °C	0.143	0.956	0.017	0.983
	45 °C	0.132	0.958	0.014	0.987

MRBC Adsorption Isotherms

The Langmuir and Freundlich models were used to further investigate MRBC sorption of Cd and Pb (Fig. 2S). The Langmuir model assumes monolayer surface sorption, while the Freundlich model is used to describe chemisorption on heterogeneous surfaces (Han *et al.* 2016). The Langmuir model was better at explaining Cd and Pb sorption by MRBC, based on the fitted results presented in Table 3. The Langmuir findings were in good agreement with the study of Bogusz *et al.* (2017), who used biomass (*Sida hermaphrodita* and wheat straw) produced biochar to adsorb Cd and Ni. In their findings, the Langmuir model was demonstrated to be the best to describe the metal sorption. In addition, Kołodyńska *et al.* (2012) reported that the pig and cow manure-based biochar were very well to fit the Langmuir model during the sorption of Cd(II) ions.

Table 3. Constants and Correlation Coefficients of Langmuir and Freundlich Models for Cd and Pb Adsorption by MRBC (at pH ~7)

Treatments	Temperature	Langmuir			Freundlich		
		K_L	Q_{max}	R^2	K_F	n	R^2
Cd	25 °C	0.248	2.396	0.964	0.267	1.394	0.802
	35 °C	0.260	2.562	0.976	0.333	1.504	0.796
	45 °C	0.249	2.971	0.985	0.397	1.529	0.812
Pb	25 °C	0.151	15.186	0.999	6.636	6.035	0.863
	35 °C	0.157	15.842	0.998	7.003	6.079	0.839
	45 °C	0.170	17.542	0.999	7.822	6.068	0.939
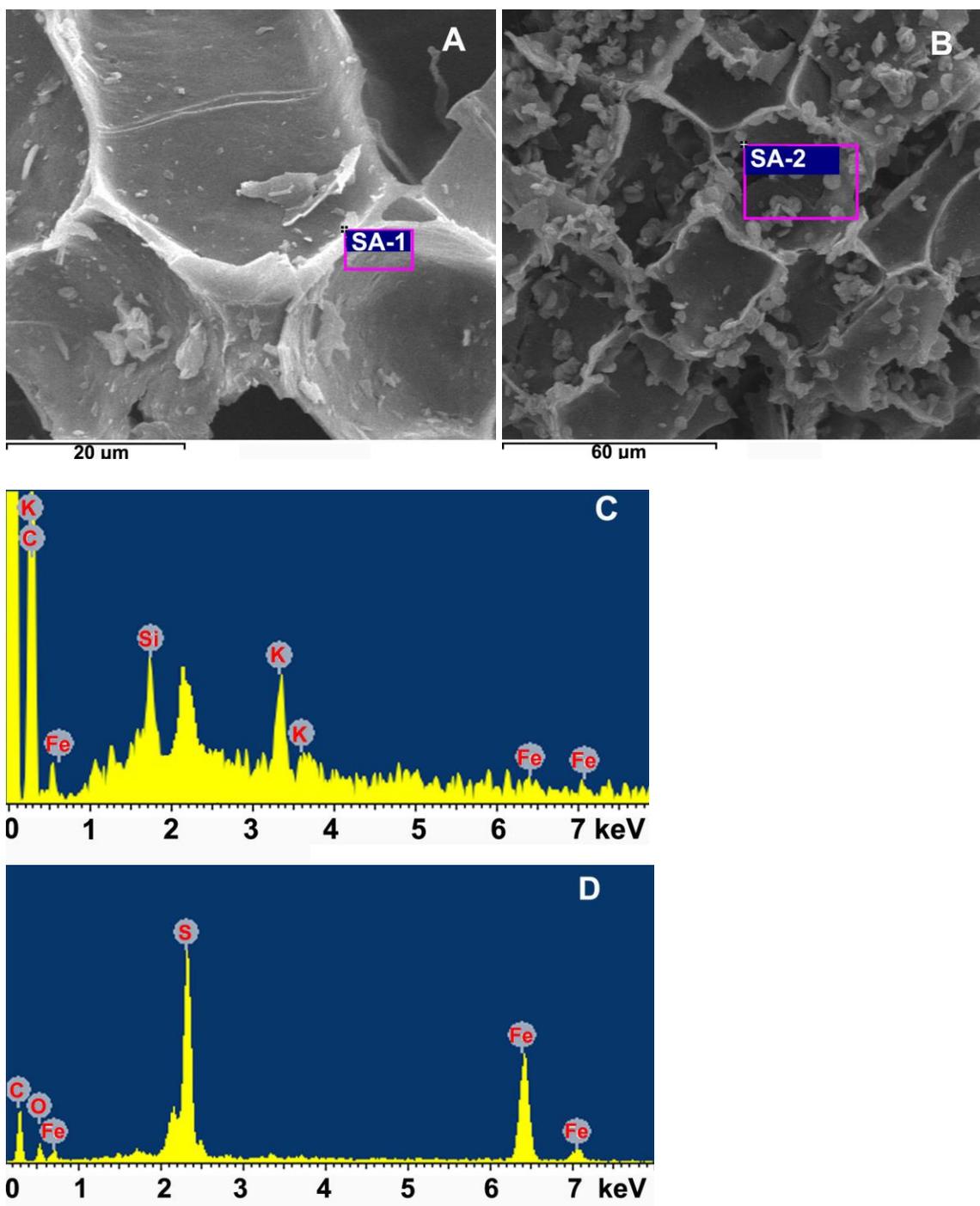
Fig. 5. SEM images of reed biochar (RBC: A) and modified reed biochar (MRBC: B); SEM-EDS spectra of RBC (C) and MRBC (D) from the areas of (SA-1) and (SA-2), respectively

As the temperature increased, the *K* value (sorption energy) increased from 0.248 to 0.260 for Cd and from 0.151 to 0.170 for Pb (Table 3). The maximum MRBC adsorption capacity increased from 25 °C (Cd, 2.40 mg g^{-1}; Pb, 15.19 mg g^{-1}) to 35 °C (Cd, 2.56 mg g^{-1}; Pb, 15.84 mg g^{-1}) to 45 °C (Cd, 2.97 mg g^{-1}; Pb, 17.54 mg g^{-1}) for Cd (by 6.9% and 24.0%, respectively) and for Pb (by 4.3% and 15.5%, respectively). The isotherms showed that the Cd and Pb sorption capacities increased with higher

temperature and initial concentration, which likely reflected a metal precipitation mechanism similar to that described by Cao *et al.* (2009). The increased sorption energy and maximum sorption capacity found here further supported the pseudo-first- and -second-order observations previously described.

RBC and MRBC Microstructure

Large microstructural changes were observed on the MRBC surface, attributed to the ferrous ammonium sulfate $[(NH_4)_2Fe(SO_4)_2]$ activation step. Specifically, a greater number of small particles containing appreciable quantities of Fe and S were observed on the MRBC surface, as compared to RBC, *via* SEM-EDS (Fig. 5B *vs.* Fig. 5A). The biochar Fe activation process likely resulted in increased surface area due to Fe precipitate formation across the biochar surface. The MRBC, with its surface activation and well-developed inner structure (as observed by comparing Fig. 5A to 5B), can offer the opportunity to adsorb more heavy metals such as Cd and Pb (Trakal *et al.* 2016). It has been suggested that Fe activation can act as a catalyst to accelerate conformational changes in biochar structure (Zhou *et al.* 2017), which likely occurred in the current study as well. The EDS spectra showed that S and Fe were more present on the MRBC than the RBC surface (Fig. 5D *vs.* Fig. 5C, respectively). Thus, it is not unreasonable to suggest that the small particles present in Fig. 5B contained both S and Fe, which developed from the biochar activation process and contributed to increased metal sorption.

CONCLUSIONS

1. Iron-activated reed biochar improved Cd and Pb sorption characteristics, such as the surface microstructure and elements content.

2. The biochar Fe activation treatment $[(NH_4)_2Fe(SO_4)_2]$ improved the presence of functional groups and microstructure surface area on MRBC, leading to enhanced Cd and Pb max sorption capacities as 2.97 mg g^{-1} and 17.5 mg g^{-1} at 45 °C on the MRBC.

3. The biochar adsorption capacities on Cd and Pb were affected by many factors. For example, the removal rate was increased to 86.8% (RBC) and 98.3% (MRBC) with the dosage at 0.8 g 50 mL^{-1}. The sorption mainly occurred in first 60 min. The MRBC sorption capacity values were increased as 41.9% (Cd) and 59.0% (Pb) at the max initial pH. The Cd and Pb removal rates were 74.6% and 76.1% on RBC and 95.9% and 88.8% on MRBC at 0.15 mm biochar.

4. Modified reed biomass biochar has the potential to be used as an efficient and eco-friendly Cd and Pb sorbent, and in the future may help reduce water-borne issues associated with metal contamination.

ACKNOWLEDGMENTS

REFERENCES CITED

Azargohar, R., and Dalai, A. (2008). "Steam and KOH activation of biochar: Experimental and modeling studies," *Micropor. Mesopor. Mat.* 110(2-3), 413-421. DOI: 10.1016/j.micromeso.2007.06.047

Bogusz, A., Nowak, K., Stefaniuk, M., Dobrowolski, R., and Oleszczuk, P. (2017). "Synthesis of biochar from residues after biogas production with respect to cadmium and nickel removal from wastewater," *J. Environ. Manage.* 201, 268-276. DOI: 10.1016/j.jenvman.2017.06.019

Bogusz, A., Oleszczuk, P., and Dobrowolski, R. (2015). "Application of laboratory prepared and commercially available biochars to adsorption of cadmium, copper and zinc ions from water," *Bioresource Technol.* 196, 540-549. DOI: 10.1016/j.biortech.2015.08.006

Bolognesi, C., Landini, E., Roggieri, P., Fabbri, R., and Viarengo, A. (1999). "Genotoxicity biomarkers in the assessment of heavy metal effects in mussels: Experimental studies," *Environ. Mol. Mutagen.* 33(4), 287-292. DOI: 10.1002/(SICI)1098-2280(1999)33:4<287::AID-EM5>3.0.CO;2-G

Cao, X., Ma, L., Gao, B., and Harris, W. (2009). "Dairy-manure derived biochar effectively sorbs lead and atrazine," *Environ. Sci. Technol.* 43(9), 3285-3291. DOI: 10.1021/es803092k

Chen, T., Zhou, Z., Han, R., Meng, R., Wang, H., and Lu, W. (2015). "Adsorption of cadmium by biochar derived from municipal sewage sludge: Impact factors and adsorption mechanism," *Chemosphere* 134, 286-293. DOI: 10.1016/j.chemosphere.2015.04.052

Cui, L., Yan, J., Yang, Y., Li, L., Quan, G., Ding, C., Chen, T., Fu, Q., and Chang, A. (2013). "Influence of biochar on microbial activities of heavy metals contaminated paddy fields," *BioResources* 8(4), 5536-5548. DOI: 10.15376/biores.8.4.5536-5548

Cui, L., Yan, J., Yang, Y., Li, L., Quan, G., Ding, C., Chen, T., Yin, C., Gao, J., and Hussain, Q. (2014). "Does biochar alter the speciation of Cd and Pb in aqueous solution?," *BioResources* 10(1), 88-104. DOI: 10.15376/biores.10.1.88-104

El-Banna, M. F., Mosa, A., Gao, B., Yin, X., Ahmad, Z., and Wang, H. (2018). "Sorption of lead ions onto oxidized bagasse-biochar mitigates Pb-induced oxidative stress on hydroponically grown chicory: Experimental observations and mechanisms," *Chemosphere* 208, 887-898. DOI:10.1016/j.chemosphere.2018.06.052

Han, L., Qian, L., Liu, R., Chen, M., Yan, J., and Hu, Q. (2017). "Lead adsorption by biochar under the elevated competition of cadmium and aluminum," *Sci. Rep.-UK* 7, Article ID 2264. DOI: 10.1038/s41598-017-02353-4

Han, Y., Cao, X., Ouyang, X., Sohi, S. P., and Chen, J. (2016). "Adsorption kinetics of magnetic biochar derived from peanut hull on removal of Cr (VI) from aqueous solution: Effects of production conditions and particle size," *Chemosphere* 145, 336-341. DOI: 10.1016/j.chemosphere.2015.11.050

Harada, M. (1995). "Minamata disease: Methylmercury poisoning in Japan caused by environmental pollution," *Crit. Rev. Toxicol.* 25(1), 1-24. DOI: 10.3109/10408449509089885

Harter, R. D., and Naidu, R. (2001). "An assessment of environmental and solution parameter impact on trace-metal sorption by soils," *Soil Sci. Soc. Am. J.* 65(3), 597–612. DOI: 10.2136/sssaj2001.653597x

Idrees, M., Batool, S., Ullah, H., Hussain, Q., Al-Wabel, M. I., Ahmad, M., Hussain, A., Riaz, M., Ok, Y.S., and Kong, J. (2018). "Adsorption and thermodynamic mechanisms of manganese removal from aqueous media by biowaste-derived biochars," *J. Mol. Liq.* 266, 373-380. DOI:10.1016/j.molliq.2018.06.049

Inaba, T., Kobayashi, E., Suwazono, Y., Uetani, M., Oishi, M., Nakagawa, H., and Nogawa, K. (2005). "Estimation of cumulative cadmium intake causing itai–itai disease," *Toxicol. Lett.* 159(2), 192-201. DOI: 10.1016/j.toxlet.2005.05.011

Inyang, M., Gao, B., Yao, Y., Xue, Y. W., Zimmerman, A. R., Pullammanappallil, P., and Cao, X. D. (2012). "Removal of heavy metals from aqueous solution by biochars derived from anaerobically digested biomass," *Bioresource Technol.* 110, 50-56. DOI: 10.1016/j.biortech.2012.01.072

Ippolito, J., Berry, C., Strawn, D., Novak, J., Levine, J., and Harley, A. (2017). "Biochars reduce mine land soil bioavailable metals," *J. Environ. Qual.* 46(2), 411-419. DOI: 10.2134/jeq2016.10.0388

Ippolito, J., Strawn, D., Scheckel, K., Novak, J., Ahmedna, M., and Niandou, M. (2012). "Macroscopic and molecular investigations of copper sorption by a steam-activated biochar," *J. Environ. Qual.* 41(4), 1150-1156. DOI: 10.2134/jeq2011.0113

Johansson, C. L., Paul, N. A., De Nys, R., and Roberts, D. A. (2016). "Simultaneous biosorption of selenium, arsenic and molybdenum with modified algal-based biochars," *J. Environ. Manage.* 165, 117-123. DOI: 10.1016/j.jenvman.2015.09.021

Jung, K. W., Lee, S. Y., and Lee, Y. J. (2018). "Hydrothermal synthesis of hierarchically structured birnessite-type MnO_2/biochar composites for the adsorptive removal of Cu (II) from aqueous media," *Bioresource Technol.* 260, 204-212. DOI:10.1016/j.biortech.2018.03.125

Kan, T., Strezov, V., and Evans, T. J. (2016). "Lignocellulosic biomass pyrolysis: A review of product properties and effects of pyrolysis parameters," *Renew. Sust. Energ. Rev.* 57, 1126-1140. DOI: 10.1016/j.rser.2015.12.185

Karunanayake, A. G., Todd, O. A., Crowley, M., Ricchetti, L., Pittman Jr, C.U., Anderson, R., Mohan, D., and Mlsna, T. (2018). "Lead and cadmium remediation using magnetized and nonmagnetized biochar from Douglas fir," *Chem. Eng. J.* 331, 480-491. DOI:10.1016/j.cej.2017.08.124

Khan, S., Cao, Q., Zheng, Y. M., Huang, Y. Z., and Zhu, Y. G. (2008). "Health risks of heavy metals in contaminated soils and food crops irrigated with wastewater in Beijing, China," *Environ. Pollut.* 152(3), 686-692. DOI: 10.1016/j.envpol.2007.06.056

Khan, S., Reid, B. J., Li, G., and Zhu, Y. G. (2014). "Application of biochar to soil reduces cancer risk *via* rice consumption: A case study in Miaoqian village, Longyan, China," *Environ. Int.* 68, 154-161. DOI: 10.1016/j.envint.2014.03.017

Kim, I. J., Kim, R. Y., Kim, J. I., Kim, H. S., Noh, H. J., Kim, T. S., Yoon, J. K., Park, G. H., Ok, Y. S., and Jung, H. S. (2015). "Feasibility study of different biochars as adsorbent for cadmium and lead," *Korean J. Soil Sci. Fert.* 48(5), 332-339. DOI: 10.7745/KJSSF.2015.48.5.332

Kołodyńska, D., Wnętrzak, R., Leahy, J. J., Hayes, M. H. B., Kwapiński, W., and Hubicki, Z. (2012). "Kinetic and adsorptive characterization of biochar in metal ions removal," *Chem. Eng. J.* 197, 295-305. DOI: 10.1016/j.cej.2012.05.025

Liang, J., Li, X., Yu, Z., Zeng, G., Luo, Y., Jiang, L., Yang, Z., Qian, Y., and Wu, H. (2017). "Amorphous MnO_2 modified biochar derived from aerobically composted

swine manure for adsorption of Pb (II) and Cd (II)," *ACS Sustain. Chem. Eng.* 5(6), 5049-5058. DOI: 10.1021/acssuschemeng.7b00434

Lima, I. M., and Marshall, W. E. (2005). "Adsorption of selected environmentally important metals by poultry manure-based granular activated carbons," *J. Chem. Technol. Biot.* 80(9), 1054-1061. DOI: 10.1002/jctb.1283

Lu, H., Zhang, W., Yang, Y., Huang, X., Wang, S., and Qiu, R. (2012). "Relative distribution of Pb^{2+} sorption mechanisms by sludge-derived biochar," *Water Res.* 46(3), 854-862. DOI: 10.1016/j.watres.2011.11.058

Lu, R. (2000). "Methods of inorganic pollutants analysis," *Soil and Agro-chemical Analysis Methods,* China Agriculture Science Press, Beijing, China, pp. 205-266

Makris, K. C., Harris, W. G., O'Connor, G. A., Obreza, T. A., and Elliott, H. A. (2005). "Physicochemical properties related to long-term phosphorus retention by drinking-water treatment residuals," *Environ. Sci. Technol.* 39(11), 4280-4289. DOI: 10.1021/es0480769

Mohan, D., Sarswat, A., Ok, Y. S., and Pittman, C. U. (2014). "Organic and inorganic contaminants removal from water with biochar, a renewable, low cost and sustainable adsorbent–A critical review," *Bioresource Technol.* 160, 191-202. DOI: 10.1016/j.biortech.2014.01.120

Qian, L., Zhang, W., Yan, J., Han, L., Gao, W., Liu, R., and Chen, M. (2016). "Effective removal of heavy metal by biochar colloids under different pyrolysis temperatures," *Bioresource Technol.* 206, 217-224. DOI: 10.1016/j.biortech.2016.01.065

Qiao, Y., Crowley, D., Wang, K., Zhang, H., and Li, H. (2015). "Effects of biochar and *Arbuscular mycorrhizae* on bioavailability of potentially toxic elements in an aged contaminated soil," *Environ. Pollut.* 206, 636-643. DOI: 10.1016/j.envpol.2015.08.029

Roberts, K. G., Gloy, B. A., Joseph, S., Scott, N. R., and Lehmann, J. (2010). "Life cycle assessment of biochar systems: Estimating the energetic, economic, and climate change potential," *Environ. Sci. Technol.* 44(2), 827-833. DOI: 10.1021/es902266r

Singh, V., Ram, C., and Kumar, A. (2016). "Physico-chemical characterization of electroplating industrial effluents of Chandigarh and Haryana Region," *J. Civil Environ. Eng.* 6, 2-6. DOI: 10.4172/2165-784X.1000237

Trakal, L., Veselská, V., Šafařík, I., Vítková, M., Číhalová, S., and Komárek, M. (2016). "Lead and cadmium sorption mechanisms on magnetically modified biochars," *Bioresource Technol.* 203, 318-324. DOI: 10.1016/j.biortech.2015.12.056

Uchimiya, M., Lima, I. M., Klasson, K. T., Chang, S., Wartelle, L. H., and Rodgers, J. E. (2010). "Immobilization of heavy metal ions (Cu^{II}, Cd^{II}, Ni^{II}, and Pb^{II}) by broiler litter-derived biochars in water and soil," *J. Agr. Food. Chem.* 58(9), 5538-5544. DOI: 10.1021/jf9044217

Wang, H., Gao, B., Wang, S., Fang, J., Xue, Y., and Yang, K. (2015). "Removal of Pb (II), Cu (II), and Cd (II) from aqueous solutions by biochar derived from $KMnO_4$ treated hickory wood," *Bioresource Technol.* 197, 356-362. DOI: 10.1016/j.biortech.2015.08.132

Wang, S., Gao, B., Li, Y., Creamer, A. E., and He, F. (2017). "Adsorptive removal of arsenate from aqueous solutions by biochar supported zero-valent iron nanocomposite: Batch and continuous flow tests," *J. Hazard. Mater.* 322, 172-181. DOI: 10.1016/j.jhazmat.2016.01.052

Wang, Z., Shen, D., Shen, F., and Li, T. (2016a). "Phosphate adsorption on lanthanum loaded biochar," *Chemosphere* 150, 1-7. DOI: 10.1016/j.chemosphere.2016.02.004

Xu, X., Cao, X., and Zhao, L. (2013). "Comparison of rice husk-and dairy manure-derived biochars for simultaneously removing heavy metals from aqueous solutions: Role of mineral components in biochars," *Chemosphere* 92(8), 955-961. DOI: 10.1016/j.chemosphere.2013.03.009

Zheng, H., Wang, Z., Deng, X., Zhao, J., Luo, Y., Novak, J., Stephen, H., and Xing, B. (2013). "Characteristics and nutrient values of biochars produced from giant reed at different temperatures," *Bioresource Technol.* 130, 463-471. DOI: 10.1016/j.biortech.2012.12.044

Zhou, N., Chen, H., Xi, J., Yao, D., Zhou, Z., Tian, Y., and Lu, X. (2017). "Biochars with excellent Pb (II) adsorption property produced from fresh and dehydrated banana peels *via* hydrothermal carbonization," *Bioresource Technol.* 232, 204-210. DOI: 10.1016/j.biortech.2017.01.074

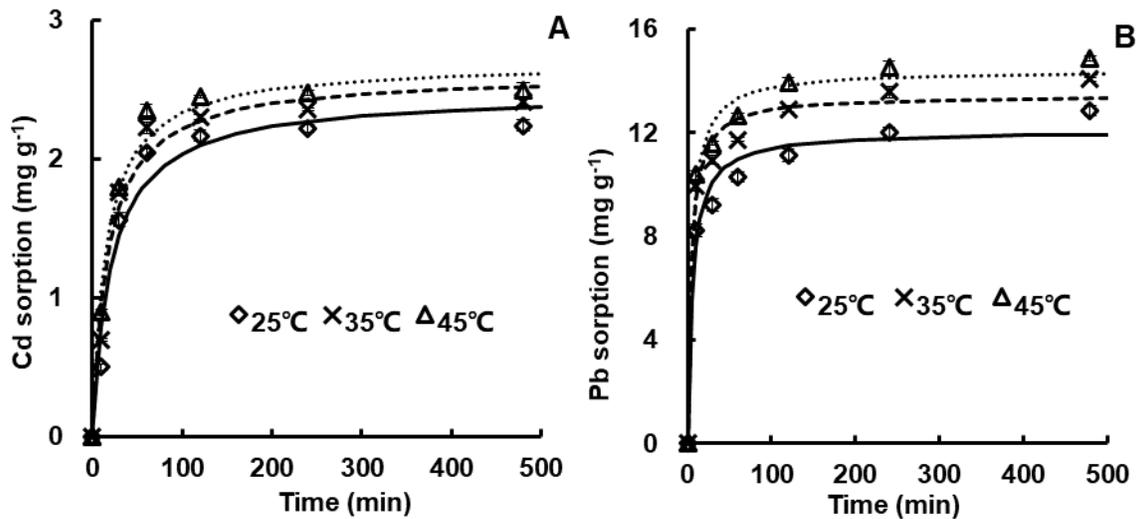## SUPPLEMENTARY INFORMATION

Fig. 1S. Adsorption kinetics of Cd (A) and Pb (B) onto MRBC following pseudo-second-order model
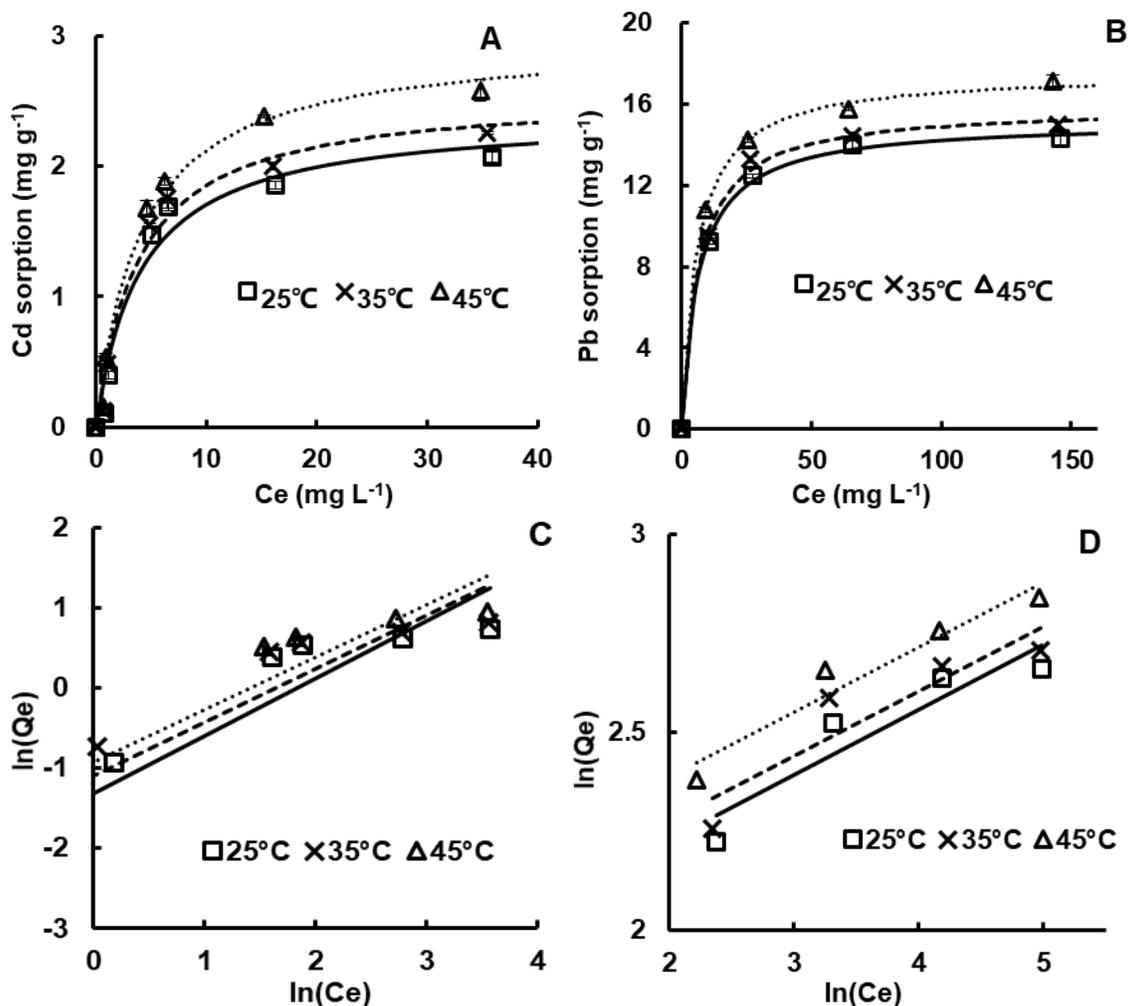

Fig. 2S. Sorption isotherms of (A, C) Cd and (B, D) Pb by MRBC with Langmuir (A, B) and Freundlich (C, D) model at different temperatures